

# On the Nonlinear Response of Lower Stratospheric Ozone to External Forces—The Inclusion of BrO<sub>x</sub> and Radiation Processes

WANG Geli\*<sup>1</sup> (王革丽), YAN Jianjun<sup>1,2</sup> (闫建军), and YANG Peicai<sup>1</sup> (杨培才)

<sup>1</sup>Key Laboratory of Middle Atmosphere and Global Environment Observation,

Institute of Atmospheric Physics, Chinese Academy of Sciences, Beijing 100029

<sup>2</sup>Meteorological Observatory in Luliang Meteorological Bureau of Shanxi Province, Lishi 033000

(Received 26 September 2011; revised 10 February 2012)

## ABSTRACT

In this paper the bromine family and radiative effects are considered in an updated box model under the framework of ozone–temperature feedback, in order to further analyze the possible behavior of atmospheric ozone in the lower mid-latitude stratosphere. Results show that this updated photochemical system can present several different solutions, within a certain domain of parameters, with fixed-point and periodic states appearing in turn. The temperature feedback effect introduced in this box model has not changed the topology of the ozone system. This result presents nonlinear characteristics of the ozone system, and possible trends in the stratospheric atmosphere between complex chemistry and radiation processes.

**Key words:** heterogeneous chemistry, ozone–temperature feedback, periodic solution

**Citation:** Wang, G. L., J. J. Yan, and P. C. Yang, 2012: On the nonlinear response of lower stratospheric ozone to external forces—The inclusion of BrO<sub>x</sub> and radiation processes. *Adv. Atmos. Sci.*, **29**(4), 855–866, doi: 10.1007/s00376-012-1177-x.

## 1. Introduction

Ozone in the stratosphere absorbs 97%–99% of the Sun's high frequency ultraviolet light, which can otherwise be damaging to life on Earth. Some chemical components of the stratosphere (e.g. ozone, water vapor, methane and volcanic ash aerosol) can affect the climate system because of their influence on the absorption and scattering of the Sun's short- and long-wave radiation, which in turn can affect the atmosphere's thermal energy structure. Climatic change can then alter the atmosphere of the stratosphere by influencing the chemical composition, density and spatial distribution of chemical processes, leading to changes in the stratospheric radiation equilibrium. The mechanisms of interactions among dynamics, chemistry and radiation processes in the stratosphere represent a very important line of research for atmospheric science today.

Studies have shown that human activity and

aerosols from volcanic eruptions exert an important influence on ozone in the stratosphere. For example, Johnston (1971) and Crutzen (1996) respectively presented a catalysis mechanism in which ozone is decomposed by nitrogen oxide. Studies have revealed that heterogeneous chemical reactions happening on an aerosol's surface play an important role in ozone depletion (Tie et al., 1994, 2006; Hofmann and Solomon, 1989; Granier and Brasseur, 1992; Tie et al., 1994; Borkov, 1995; Li et al., 2005; Tie et al., 2006). Furthermore, studies related to the mesosphere have shown the existence of multiple steady states (White and Dietz, 1984; Yang and Brasseur, 1994; Konovalov et al., 1999; Yang and Brasseur, 2001, 2004). Subsequently, Wang and Yang (2006, 2007) improved the heterogeneous chemical system to one that consisted of nineteen species belonging to five chemical families. Their results showed that, just in terms of aerosols, they are not an important factor in determining the nonlinear behavior of the heterogeneous system under the cur-

\*Corresponding author: WANG Geli, wgl@mail.iap.ac.cn

rent conditions. However, if the heterogeneous system is controlled together by aerosols and a source of reactive chlorine ( $\text{ClO}_x$ ), or a source of reactive nitrogen ( $\text{NO}_x$ ), the heterogeneous chemistry may produce a significant influence on nonlinear behavior of the system through chlorine and nitrogen chemistry. Furthermore, in some parameter ranges, it can be presented as the existence of multi-equilibrium solutions, which could produce a folding transition.

However, the above studies did not consider the influence of bromine. It is known that bromine is a widely existing and well-used element in the troposphere and its transportation can also affect stratospheric ozone (Fisher et al., 1994; Tie and Brasseur, 1996). The main sources of bromine are methyl bromide and halon. Methyl bromide derives from both natural and anthropogenic sources. Natural sources include the sea and soil emissions, and anthropogenic sources are generally industrial and agricultural emissions. Halons are commonly used as reagents in fire extinguishers and, in the troposphere, are too stable to cause pollution. However, when transported to the stratosphere, halons can photolyze to leave free radicals (Br, BrO), which have a destructive effect on stratospheric ozone, like chloride (Weinberg et al., 1994). In addition, bromine can not only catalyze the destruction of ozone, but also react with other chemicals (nitrogen, chlorine, hydrogen family). It has been noted that in the Atlantic area about 2% of ozone reduction can be ascribed to bromine. Moreover, bromine is possibly more serious for ozone destruction in the Northern Hemisphere. Thus, the role of bromine cannot be underestimated (WMO, 2007).

In recent decades, in the case of global warming, how the stratospheric ozone photochemical system could be altered is becoming an important topic of concern (Hu et al., 2009). To date, middle stratospheric general circulation models have already made important progress in simulating the stratosphere (Tie et al., 2006; Tian et al., 2009, Bi et al., 2011); however, simplified physics-based box models are more efficient in terms of computing resources than complex general circulation models, and are more realistic, physically, than statistical models.

Therefore, the present work aims to extend the previous studies of Wang and Yang (2006, 2007). In this paper, we improve the original box model through introducing the bromine family and radiation equation to analyze the behavior of the lower stratospheric photochemical system in response to external forces by anthropogenic and natural perturbations, such as enhanced atmospheric abundances of sulfate aerosols and reactive nitrogen, chlorine and bromine, on the conditions of radiative feedback. Results will illustrate

the nonlinear behavior of the ozone system, as well as the possible latent trend of development in the stratospheric atmosphere between complex chemistry and radiation processes.

The new box model is described in section 2, and in section 3 we evaluate the response of the photochemical system to external forcing strengthened by nitrogen chlorine and bromine with aerosol surface area density. Finally, in section 4, a discussion of the results is presented.

## 2. Description of the present model

In this paper, a new ozone heterogeneous photochemical box model is established at 18 km altitude which can exhibit the average circumstances of the lower stratospheric atmosphere for equinoctial conditions at 40°N. The model consists of six chemical families: oxygen [ $\text{O}_3$ , O(3p), O(1D),  $\text{O}_2$ ], hydrogen (OH,  $\text{HO}_2$ ), nitrogen (NO,  $\text{NO}_2$ ,  $\text{NO}_3$ ,  $\text{N}_2\text{O}_5$ ,  $\text{HNO}_3$ ,  $\text{HNO}_4$ ), chlorine (Cl, ClO,  $\text{ClO}_2$ ,  $\text{Cl}_2\text{O}_2$ , HCl, HOCl,  $\text{ClONO}_2$ ), bromide (Br, BrO, HBr,  $\text{BrONO}_2$ ) and carbon ( $\text{CH}_4$ , CO). For the atmospheric constituents  $\text{O}_2$  and  $\text{H}_2\text{O}$ , whose lifetime in the stratosphere is longer, their concentration is often referred to as constant. The most important photolysis and chemical reactions chosen in this box model are given in Tables 1 and 2.

**Table 1.** Photolysis reactions used in this heterogeneous model.

	Reactions
1	$\text{O}_2 + h\nu \rightarrow \text{O} + \text{O}$
2	$\text{O}_3 + h\nu \rightarrow \text{O}_2 + \text{O}(1\text{D})$
3	$\text{O}_3 + h\nu \rightarrow \text{O}_2 + \text{O}$
4	$\text{H}_2\text{O} + h\nu \rightarrow \text{H} + \text{OH}$
5	$\text{H}_2\text{O}_2 + h\nu \rightarrow 2\text{OH}$
6	$\text{NO}_2 + h\nu \rightarrow \text{NO} + \text{O}$
7	$\text{NO}_3 + h\nu \rightarrow \text{NO} + \text{O}_2$
8	$\text{NO}_3 + h\nu \rightarrow \text{NO}_2 + \text{O}$
9	$\text{N}_2\text{O}_5 + h\nu \rightarrow \text{NO}_2 + \text{NO}_3$
10	$\text{HNO}_3 + h\nu \rightarrow \text{OH} + \text{NO}_2$
11	$\text{HO}_2\text{NO}_2 + h\nu \rightarrow \text{HO}_2 + \text{NO}_2$
12	$\text{ClONO}_2 + h\nu \rightarrow \text{ClO} + \text{NO}_2$
13	$\text{ClONO}_2 + h\nu \rightarrow \text{Cl} + \text{NO}_3$
14	$\text{HOCl} + h\nu \rightarrow \text{OH} + \text{Cl}$
15	$\text{ClO}_2 + h\nu \rightarrow \text{O} + \text{ClO}$
16	$\text{Cl}_2\text{O}_2 + h\nu \rightarrow 2\text{Cl} + \text{O}_2$
17	$\text{BrO} + h\nu \rightarrow \text{Br} + \text{O}$
18	$\text{HOBr} + h\nu \rightarrow \text{Br} + \text{OH}$
19	$\text{BrONO}_2 + h\nu \rightarrow \text{Br} + \text{NO}_3$
20	$\text{BrONO}_2 + h\nu \rightarrow \text{BrO} + \text{NO}_2$

**Table 2.** Chemical reactions used in this heterogeneous model.

	Reactions
1	$O+O_2+M \rightarrow O_3+M$
2	$O+O+M \rightarrow O_2+M$
3	$O+O_3 \rightarrow 2O_2$
4	$O(1D)+O_3 \rightarrow 2O_2$
5	$O(1D)+N_2 \rightarrow O+N_2$
6	$O(1D)+O_2 \rightarrow O+O_2$
7	$O(1D)+H_2O \rightarrow 2OH$
8	$O(1D)+CH_4 \rightarrow CO+2H_2O$
9	$OH+CH_4 \rightarrow CO+2H_2O+HO_2$
10	$OH+O_3 \rightarrow O_2+HO_2$
11	$OH+CO \rightarrow CO_2+HO_2$
12	$OH+OH \rightarrow H_2O+O$
13	$OH+OH+M \rightarrow H_2O_2+M$
14	$OH+HO_2 \rightarrow H_2O+O_2$
15	$HO_2+O \rightarrow O_2+OH$
16	$HO_2+O_3 \rightarrow 2O_2+OH$
17	$HO_2+HO_2 \rightarrow H_2O_2+O_2$
18	$HO_2+HO_2+M \rightarrow H_2O_2+O_2+M$
19	$OH+H_2O_2 \rightarrow H_2O+HO_2$
20	$O+H_2O_2 \rightarrow OH+HO_2$
21	$NO+O+M \rightarrow NO_2+M$
22	$NO+O_3 \rightarrow NO_2+O_2$
23	$NO+HO_2 \rightarrow NO_2+OH$
24	$NO_2+O \rightarrow NO+O_2$
25	$NO_2+O+M \rightarrow NO_3+M$
26	$NO_2+O_3 \rightarrow NO_3+O_2$
27	$NO_2+OH+M \rightarrow HNO_3+M$
28	$HNO_3+OH \rightarrow H_2O+NO_3$
29	$NO_2+HO_2+M \rightarrow HO_2NO_2+M$
30	$HO_2NO_2+M \rightarrow NO_2+HO_2+M$
31	$HO_2NO_2+OH \rightarrow NO_2+H_2O+O_2$
32	$NO_2+NO_3+M \rightarrow N_2O_5+M$
33	$N_2O_5+M \rightarrow NO_2+NO_3+M$
34	$NO_3+O \rightarrow NO_2+O_2$
35	$NO_3+OH \rightarrow NO_2+HO_2$
36	$NO_3+HO_2 \rightarrow OH+NO_2+O_2$
37	$NO_3+HO_2 \rightarrow HNO_3+O_2$
38	$NO_3+NO \rightarrow 2NO_2$
39	$Cl+O_3 \rightarrow ClO+O_2$
40	$Cl+HO_2 \rightarrow HCl+O_2$
41	$Cl+HO_2 \rightarrow ClO+OH$
42	$Cl+H_2O_2 \rightarrow HCl+HO_2$
43	$Cl+NO_3 \rightarrow NO_2+ClO$
44	$Cl+CH_4 \rightarrow HCl+CO+HO_2+H_2O$
45	$ClO+O \rightarrow Cl+O_2$
46	$ClO+OH \rightarrow Cl+HO_2$
47	$ClO+OH \rightarrow HCl+O_2$
48	$ClO+HO_2 \rightarrow HOCl+O_2$
49	$ClO+NO \rightarrow NO_2+Cl$
50	$ClO+NO_2+M \rightarrow ClONO_2+M$
51	$ClONO_2+O \rightarrow ClO+NO_3$
52	$ClONO_2+OH \rightarrow HOCl+NO_3$
53	$ClO+NO_3 \rightarrow Cl+NO_2+O_2$
54	$ClO+ClO \rightarrow Cl+OClO$
55	$OClO+O \rightarrow ClO+O_2$
56	$OClO+OH \rightarrow HOCl+O_2$
57	$OClO+NO \rightarrow ClO+NO_2$
58	$OClO+Cl \rightarrow ClO+ClO$

**Table 2 (Continued).**

	Reactions
59	$ClO+ClO+M \rightarrow Cl_2O_2+M$
60	$Cl_2O_2+M \rightarrow 2ClO+M$
61	$HCl+O(1D) \rightarrow Cl+OH$
62	$HCl+O \rightarrow Cl+OH$
63	$HCl+OH \rightarrow Cl+H_2O$
64	$HOCl+O \rightarrow ClO+OH$
65	$HOCl+OH \rightarrow ClO+H_2O$
66	$Br+O_3 \rightarrow BrO+O_2$
67	$Br+HO_2 \rightarrow HBr+O_2$
68	$Br+OClO \rightarrow BrO+ClO$
69	$BrO+O \rightarrow Br+O_2$
70	$BrO+OH \rightarrow Br+HO_2$
71	$BrO+HO_2 \rightarrow HOBr+O_2$
72	$BrO+NO \rightarrow Br+NO_2$
73	$BrO+NO_2+M \rightarrow BrONO_2+M$
74	$BrO+ClO \rightarrow OClO+Br$
75	$BrO+ClO \rightarrow Br+Cl+O_2$
76	$BrO+BrO \rightarrow 2Br+O_2$
77	$HBr+O(1D) \rightarrow Br+OH$
78	$HBr+O \rightarrow Br+OH$
79	$HBr+OH \rightarrow Br+H_2O$
80	$HOBr+O \rightarrow BrO+OH$

The expression for the photolysis reaction rate is

$$J_i(z; Z) = 4\pi \int \sigma_i(\lambda) \varepsilon_i(\lambda) I(\lambda; z; Z) d\lambda. \quad (1)$$

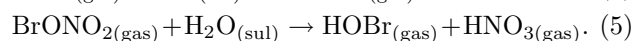
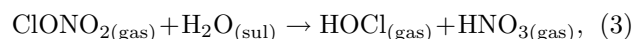
Here,  $\lambda$  is the wavelength,  $z$  represents the log-pressure altitude,  $Z$  represents the solar zenith angle. This photolysis rate  $J(s^{-1})$  for a given species  $i$  is proportional to the solar actinic flux  $4\pi I$ , the absorption cross section  $\sigma_i(cm^{-2})$  and the quantum efficiency  $\varepsilon_i$ .

For the two-body chemical reaction rate:

$$k(T) = A_r \exp\left(-\frac{E}{R}\right) \left(\frac{1}{T}\right), \quad (2)$$

where  $A_r$  is the Arrhenius constant,  $R$  is the gas constant, and  $E$  represents the activation energy.

Moreover, the most important heterogeneous chemical reactions happen in the lower stratospheric aerosol layer, and are as follows (Rodriguez et al., 1991):



Their reaction rates can be expressed as:

$$K_h = \gamma VA/4, \quad (6)$$

where  $A$  stands for the total surface area of aerosol in unit volume (in fact,  $A/4$  is the total impact area),  $\gamma$  is the surface reaction probability between a gas molecule and an aerosol particle and  $V$  is the mean molecular speed.  $V$  is usually taken as a constant at  $2.08 \times 10^4 \text{ cm s}^{-1}$ . Measurements in the laboratory indicate  $\gamma_2 \approx 0.14$ ,  $\gamma_3 \approx 0.6$  and  $\gamma_1$  is dependent on temperature and the ratio between  $\text{H}_2\text{SO}_4$  and  $\text{H}_2\text{O}$  in weight (Hanson and Mauersberger, 1988; Tolbert et al., 1988). In the calculation of  $\gamma_1$ , the following formula is used:

$$\gamma_1 = 10^{1.86 - 0.0747\omega}, \quad (7)$$

which is from the 2-D photochemical model of the NCAR (Theresa et al., 1998). Here,  $\omega$  is the weight percentage of sulfuric acid in aerosol, which depends on air temperature and moisture content.

The most important module added in this updated model is a radiation scheme. In a 2-D convection model, the temperature equation is often expressed as:

$$\frac{\partial \bar{\theta}}{\partial t} + \bar{v}^* \frac{\partial \bar{\theta}}{\partial y} + \bar{w}^* \frac{\partial \bar{\theta}}{\partial z} = Q_S + Q_{\text{IR}} + D_\theta, \quad (8)$$

Where  $\bar{\theta}$  is zonally-averaged potential temperature,  $\bar{v}^*$  is meridional residual wind velocity,  $\bar{w}^*$  is vertical residual wind.

The terms on the left of the above equation are the local variability of potential temperature, the horizontal and vertical advection, respectively. On the right are solar heating, radiation cooling and friction heating. Since movement is not involved in this box model, the above equation can be simplified as:

$$\frac{d\bar{\theta}}{dt} = Q_S + Q_{\text{IR}} + \text{Const}, \quad (9)$$

Let  $Q_{\text{net}} = Q_S + Q_{\text{IR}}$ , solving this differential equation then

$$\bar{\theta}(n) = Q_{\text{net}}(n) \times \Delta t - Q_{\text{net}}(n-1) \times \Delta t + \bar{\theta}(n-1). \quad (10)$$

Here  $n$  means integration step. Turning the potential temperature to absolute temperature with

$$\bar{T} = \bar{\theta} \left( \frac{1000}{p} \right)^{-0.286}. \quad (11)$$

$\bar{T}$  is zonally-averaged temperature. Since the present model is set in the lower stratosphere at around 18 km, then  $p$  is given as 83.4 hPa.

The following equation is for calculating the heating rate, and we only consider contributions by  $\text{O}_2$  and  $\text{O}_3$  (Theresa et al., 1998):

$$Q_{\text{S}_{\text{O}_2}}(z; Z) = 4\pi \frac{6 \times 10^{23}}{c_p m_{\text{air}} [M]} [\text{O}_2] \times \int_{\lambda} \frac{hc}{\lambda} \sigma_{\text{O}_2} I(\lambda; z, Z) d\lambda, \quad (12)$$

$$Q_{\text{S}_{\text{O}_3}}(z; Z) = 4\pi \frac{6 \times 10^{23}}{c_p m_{\text{air}} [M]} [\text{O}_3] \times \int_{\lambda} \frac{hc}{\lambda} \sigma_{\text{O}_3} I(\lambda; z, Z) d\lambda, \quad (13)$$

where  $m_{\text{air}}$  is the molecular weight of air,  $[M]$  is the air number density,  $[\text{O}_2]$  is the  $\text{O}_2$  number density and  $[\text{O}_3]$  the ozone number density,  $h$  is Planck constant and  $c$  is light velocity,  $\sigma_{\text{O}_2}$  and  $\sigma_{\text{O}_3}$  is the absorption cross section of  $\text{O}_2$  and  $\text{O}_3$ , respectively.  $c_p$  is the specific heat at constant pressure

For calculating the infrared radiation, the following scheme is used (Briegleb, 1992):

$$Q_{\text{ir}} = \frac{g}{c_p} \frac{F^-(p_{k+1}) - F^+(p_{k+1}) - F^-(p_k) + F^+(p_k)}{p_{k+1} - p_k}, \quad (14)$$

where  $F^+$  and  $F^-$  is for the upward and downward long-wave fluxes,  $p$  is for pressure,  $k$  is for layer.

This is a zero-dimension box model, which does not involve vertical and horizontal variability; therefore, it needs to make a hypothesis that the radiant flux from the upper and lower level is stable. However, with the atmospheric density changing, the radiant flux can be affected by the outside, and thus affects the radiation cooling rate like  $\text{O}_3$ ,  $\text{H}_2\text{O}$ ,  $\text{CH}_4$  of this level, which in turn can change the chemical reaction process. Thus, a stratospheric chemical box model including radiation feedback is established.

Sources of reactive nitrogen, chlorine and bromide (denoted as  $S_N$ ,  $S_{\text{Cl}}$ , and  $S_b$ ; units:  $\text{cm}^{-3} \text{ s}^{-1}$ ; similar hereinafter) arise from human activity, such as the photo-oxidation of nitrous oxide ( $\text{N}_2\text{O}$ ) and the photolysis of chlorofluorocarbons (CFCs) and halons, sinks of nitrogen; chlorine and bromide are caused by wet scavenging processes by  $\text{HNO}_3$ ,  $\text{HBr}$ ,  $\text{HCl}$  and  $\text{CO}$  (Yang and Brasseur, 2001; Potter et al., 1995). In addition, because the atmospheric constituent  $\text{CH}_4$  cannot be directly obtained by chemical and photolysis reactions in the stratosphere, in order to compensate for its loss, one source of  $\text{CH}_4$  (denoted as  $S_{\text{CH}_4}$ ) is added in this model, which is produced by surface emissions and could be transported to the stratosphere by some dynamic processes. All the current sources and losses used in this model are given in Table 3. The photochemical states are the average between the daytime

**Table 3.** Parameters used in the present heterogeneous model.

Parameters	Current value
first-order loss rate constants for HNO <sub>3</sub>	$3.2 \times 10^{-9} \text{ s}^{-1}$
first-order loss rate constants for HCl	$8.0 \times 10^{-9} \text{ s}^{-1}$
first-order loss rate constants for CO	$4.5 \times 10^{-8} \text{ s}^{-1}$
first-order loss rate constants for HBr	$9.4 \times 10^{-8} \text{ s}^{-1}$
source strength of CH <sub>4</sub>	$1.3 \times 10^3 \text{ cm}^{-3} \text{ s}^{-1}$
strength of ClO <sub>x</sub>	$20 \text{ cm}^{-3} \text{ s}^{-1}$
source strength of NO <sub>x</sub>	$20 \text{ cm}^{-3} \text{ s}^{-1}$
source strength of BrO <sub>x</sub>	$0.428 \text{ cm}^{-3} \text{ s}^{-1}$

and night-time solutions. Similar to Wang and Yang (2006, 2007), the solution of the numerically “stiff” nonlinear first-order differential equations is solved by using the Gear algorithm (Gear, 1969).

In order to verify the present model, we integrated the updated box model with the current source and sink values in Table 3. The simulation results are shown in Table 4. Due to lacking of observational data for chemical components in the stratosphere, those chemical components have to be compared with other models. It is noted that all the corresponding species have the same values in orders of magnitude, although some small differences exist. Thus, the present model can capture the most important chemical processes that influence stratospheric ozone and can better describe the average characteristics of atmospheric components in the lower stratosphere.

By using the updated heterogeneous chemical box model in the lower stratosphere, we attempt in the following to analyze the behavior of the lower stratospheric photochemical system in response to enhanced reactive nitrogen chlorine and bromide sources along with atmospheric abundances of sulfate aerosols. Because the observations show that, when the Mount Pinatubou event occurred, the aerosol concentrations reached about 10–100 (units:  $10^{-8} \text{ cm}^{-3}$ ; neglected hereafter) (Prather, 1992; McCormick and Veiga, 1992), one cannot ignore the possibility that we would see more of an increase under some extreme conditions.

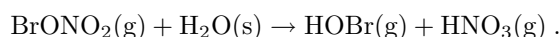
### 3. Results

In this section, we assume that aerosol surface area density  $A$  and  $S_N$ , (or  $S_{cl}$  or  $S_b$ ) are simultaneously changed. This is equivalent to discussing the behavior of the system in 2-D parameter space. The ranges of the parameters  $S_N$  (or  $S_{cl}$  or  $S_b$ ) change from 1 to 28 times, and  $A$  is given by [1, 150]. The other parameters remain at their current values, and it is noted from all the solutions that no time-dependent solution is found except equilibrium solutions in this parameter domain.

#### 3.1 Response to the situation that both $S_N$ and $A$ change

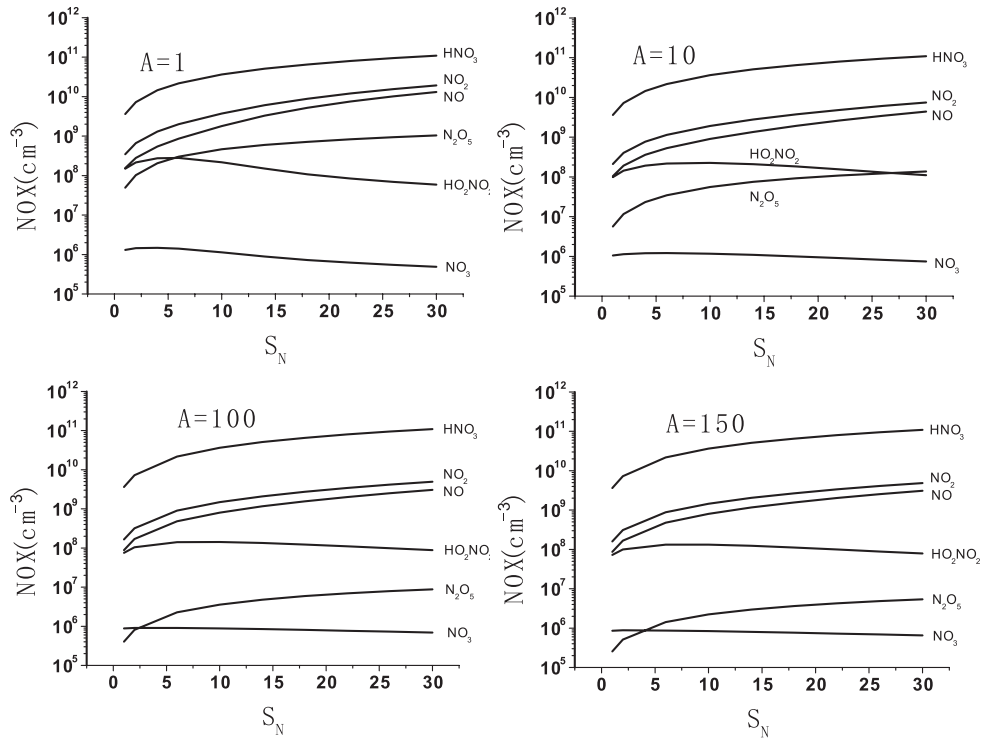
Figure 1 gives the dependence of the states of the NO<sub>x</sub> system on  $A$  and the reactive nitrogen resource  $S_N$ , which shows concentrations of the nitrogen family of this system when the source strength of reactive nitrogen  $S_N$  is changing from 1 to 28 times, and  $A$  is fixed at 1, 10, 100 and 150. It shows that densities of components like NO, NO<sub>2</sub>, N<sub>2</sub>O<sub>5</sub> rise continuously with an increasing of  $S_N$ ; the number densities of HO<sub>2</sub>NO<sub>2</sub> and NO<sub>3</sub> firstly decrease then increase, under different aerosol conditions, and the number densities of all the nitrogen family decrease, especially for N<sub>2</sub>O<sub>5</sub>.

Figure 2 gives the dependence of the states of the BrO<sub>x</sub> system on  $A$  and the reactive nitrogen resource  $S_N$ , which shows the solutions of the bromine family of this system when  $S_N$  is changing from 1 to 28 times, and  $A$  is fixed at 1, 10, 100 and 150. It shows that under identical aerosol conditions, the number density of bromine increases with increasing  $S_N$ . With the same value of  $S_N$ , densities of BrO, HOBr increase, but Br and BrONO<sub>2</sub> decrease with an increase of  $A$ ; the density BrONO<sub>2</sub> decreases by 10 orders of magnitude. Meanwhile, the density of HOBr increases by approximately 10 orders of magnitude. This could be attributed to the third heterogeneous chemical reaction:

**Table 4.** Modeling results of some species for the current state ( $\text{cm}^{-3}$ ).

	O <sub>3</sub>	HO <sub>x</sub>	NO <sub>x</sub>	ClO <sub>x</sub>	BrO <sub>x</sub>	HNO <sub>3</sub>	ClONO <sub>2</sub>	BrONO <sub>2</sub>	CH <sub>4</sub>
(1)	$2.55 \times 10^{12}$	$7.43 \times 10^6$	$2.66 \times 10^9$	$1.57 \times 10^6$	—	$9.08 \times 10^9$	$9.3 \times 10^7$	—	$4.29 \times 10^{12}$
(2)	$3.48 \times 10^{12}$	$1.87 \times 10^6$	$2.76 \times 10^9$	$1.25 \times 10^6$	—	$2.21 \times 10^{10}$	$9.01 \times 10^7$	—	$3.02 \times 10^{12}$
(3)	$2.96 \times 10^{12}$	$6.15 \times 10^6$	$5.83 \times 10^8$	$1.48 \times 10^7$	$4.27 \times 10^6$	$4.49 \times 10^9$	$2.12 \times 10^8$	$5.93 \times 10^6$	$4.30 \times 10^{12}$
(4)	$2.60 \times 10^{12}$	$2.87 \times 10^6$	$5.06 \times 10^8$	$1.14 \times 10^6$	$7.63 \times 10^6$	$3.64 \times 10^9$	$1.18 \times 10^7$	$7.14 \times 10^6$	$2.98 \times 10^{12}$

(1) Simulations by Orlando et al. (1991); (2) Results from Wang and Yang (2007); (3) By model of SOCRATES/NCAR; (4) Results provided by this model.



**Fig. 1.** Dependence of the states of the  $\text{NO}_x$  system on  $A$  (units:  $10^{-8} \text{ cm}^{-1}$ ) and the reactive nitrogen resource  $S_N$  ( $\text{cm}^{-3} \text{ s}^{-1}$ ).

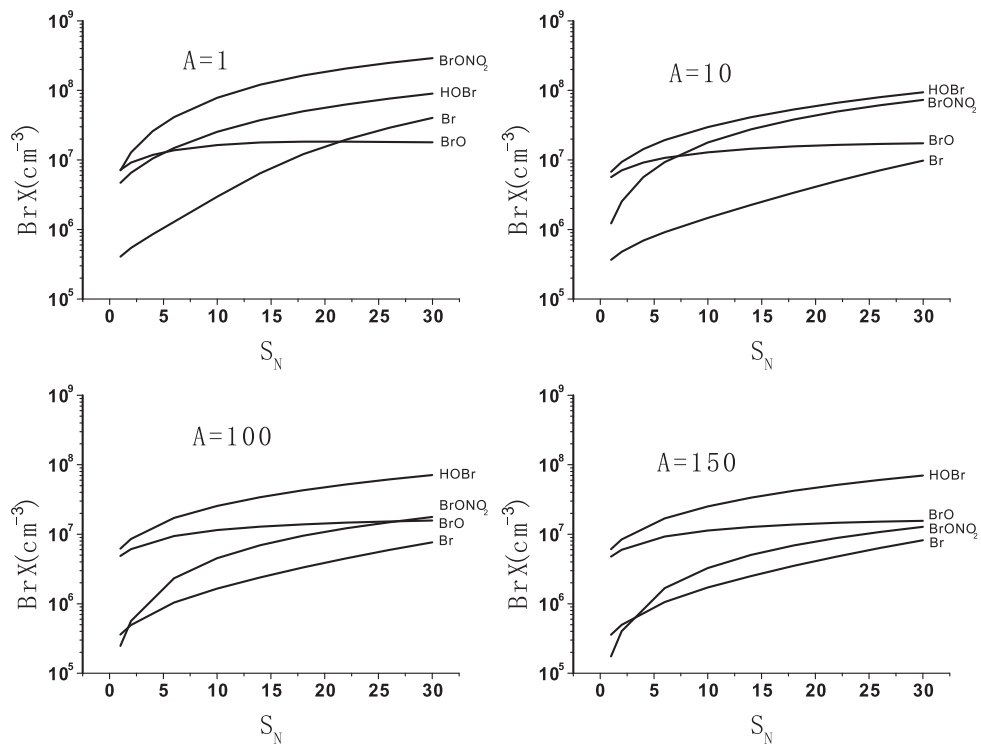


**Fig. 2.** Dependence of the states of the  $\text{Br}_x$  system on  $A$  and the reactive nitrogen resource  $S_N$ .

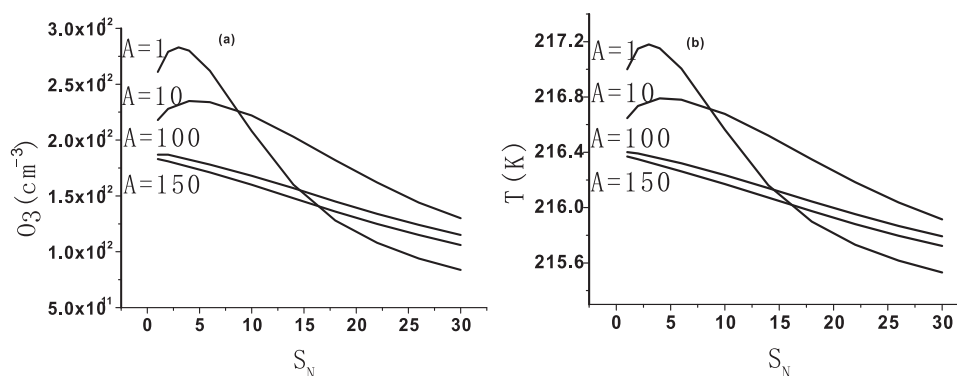


**Fig. 3.** Dependence of the states of the ozone system (a) and temperature (b) on  $A$  and the reactive nitrogen resource  $S_N$ .

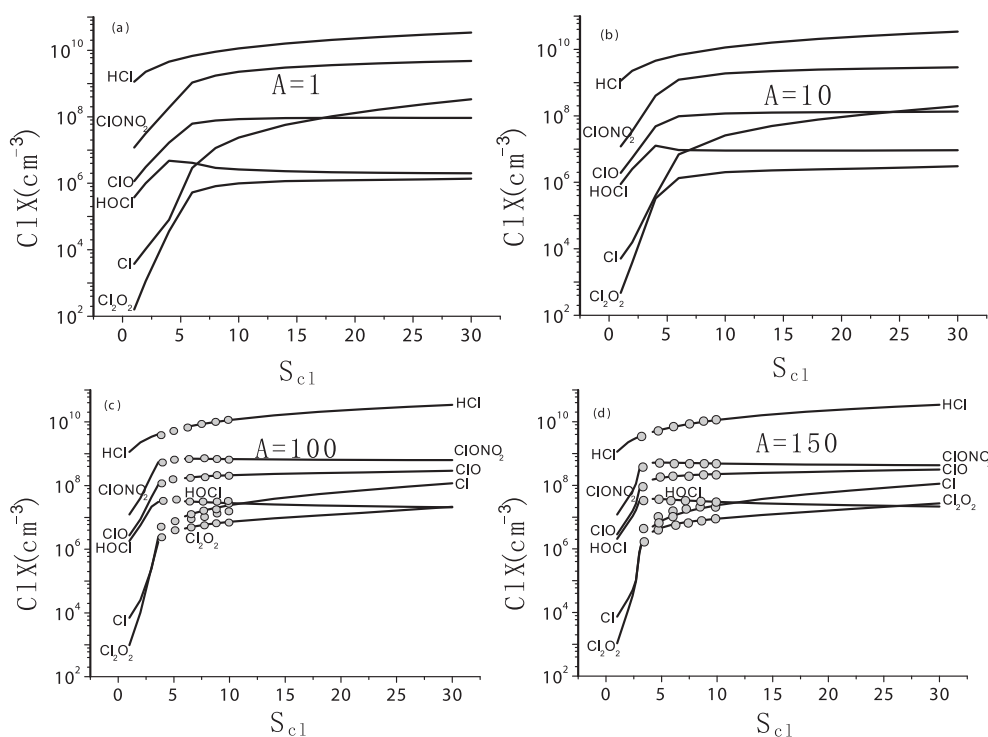
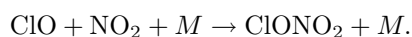
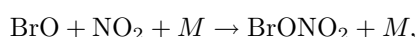


**Fig. 4.** Dependence of the states of the  $Cl_x$  system on  $A$  and the reactive chlorine resource  $S_{Cl}$ .

Increasing aerosol abundance may enhance the concentration of HOBr, compared with the results of Wang and Yang (2007). Under the same emissions, introducing bromide can change the proportion of nitrogen oxide and chlorine oxide. In other words, nitrogen oxide reduces and chlorine oxide enhances in the new model. Therefore:



Under the same emissions, by introducing bromine,  $NO_2$  can decrease, leading to a reduction of ClO,

BrO into  $ClONO_2$ ,  $BrONO_2$ , and thus the net results caused by the heterogeneous chemistry are enhancing the reactive chlorine and reducing reactive nitrogen for depleting ozone.

Figure 3a gives the density of  $O_3$  dependence with  $S_N$  and  $A$ , which shows the concentration of  $O_3$  in this photochemical system when  $S_N$  is changing from 1 to 28 times, with  $A$  fixed at 1, 10, 100 and 150. It is noted that when  $A$  is lower, especially with  $A = 1$  and  $A = 10$ , the density of  $O_3$  firstly increases then decreases rapidly along with an increasing of  $S_N$ . When  $A = 100$  or  $A = 150$ , the density of  $O_3$  decreases with  $S_N$ . Under the same emission conditions of  $S_N$ , we can

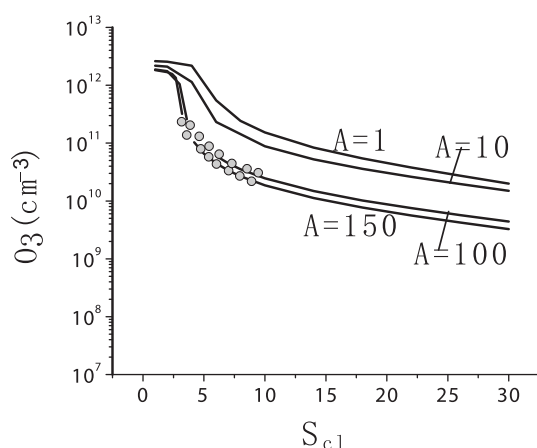


**Fig. 5.** Dependence of the states of the ozone system on  $A$  and the reactive chlorine resource  $S_{cl}$ .

see that the density of  $O_3$  decreases with an increasing of  $A$ , because increasing aerosol can cause the nitrogen oxide to be transformed to  $HNO_3$ , the chloride oxide and the bromide to enhance accordingly, and then increase the chance of ozone loss. Temperature depends on  $S_N$  and  $A$  has a similar topology structure to ozone, shown in Fig. 3b.

### 3.2 Response to the situation that both $S_{cl}$ and $A$ change

Figure 4 gives the dependence of the states of the  $Cl_x$  system on  $A$  and the reactive chlorine resource  $S_{cl}$ , which shows the solutions of the chloride family of this system when  $S_{cl}$  is changing from 1 to 28 times, with  $A$  fixed at 1, 10, 100 and 150. It can be seen that the solutions of the system in Fig. 4a have similar structure to that shown in Fig. 4b. On the whole, all densities of the chloride family increase with  $S_{cl}$ . However, when  $A = 100$  (in Fig. 4c), some dramatic changes occur, increasing with  $S_{cl}$  for each composition a supercritical Hopf bifurcation takes place, the original equilibrium solution loses its stability and a new stable periodic solution appears. After  $S_{cl}$  increases to about 10 times, another equilibrium state takes place; when  $A = 150$ , shown in Fig. 4d, it has a similar topology to that with  $A = 100$ .

This is also clearly shown in Fig. 5, which describes the structure of the density of ozone dependence with  $S_{cl}$  and  $A$ , and shows ozone concentration of this photochemical system when  $S_{cl}$  is changing from 1 to 28 times, with  $A$  fixed at 1, 10, 100 and 150. It shows that increasing with  $S_{cl}$ , the density of ozone decreases with  $S_c$  and  $A$ . When  $A=100$  and  $S_{cl}$  increases to near 3.6 times from the current value, a supercritical Hopf bifurcation takes place, the original equilibrium solution loses stability and the ozone system moves to a new stable periodic solution. Then, another equilibrium

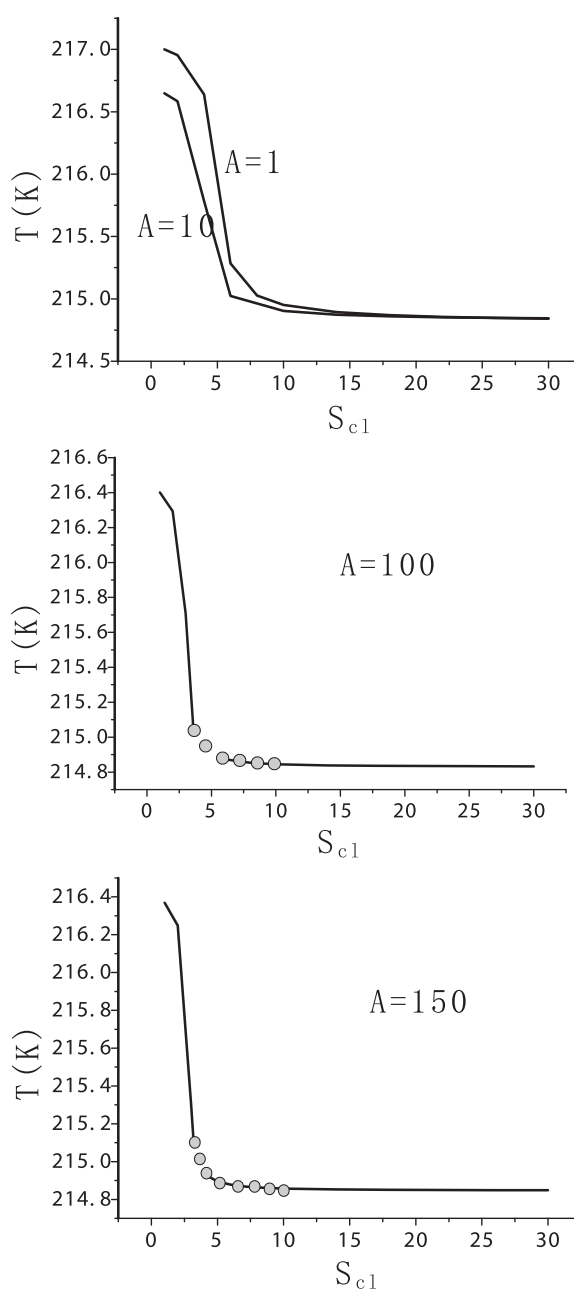


**Fig. 6.** Dependence of the states of temperature on  $A$  and the reactive chlorine resource  $S_{cl}$ .

state takes place after  $S_c$  increases to about 10 times; when  $A = 150$ , it has a similar topology to the system, but the sensitive value that leads to Hopf bifurcation from an equilibrium solution to a periodic one is about 3.2 times that of the current value, which is a bit ahead of that when  $A = 100$ .

A similar topology can also be seen in temperature dependence with  $S_{cl}$  when  $S_{cl}$  is changing from 1 to 28 times, with  $A$  fixed at 1, 10, 100 and 150 times, as shown in Fig. 6.



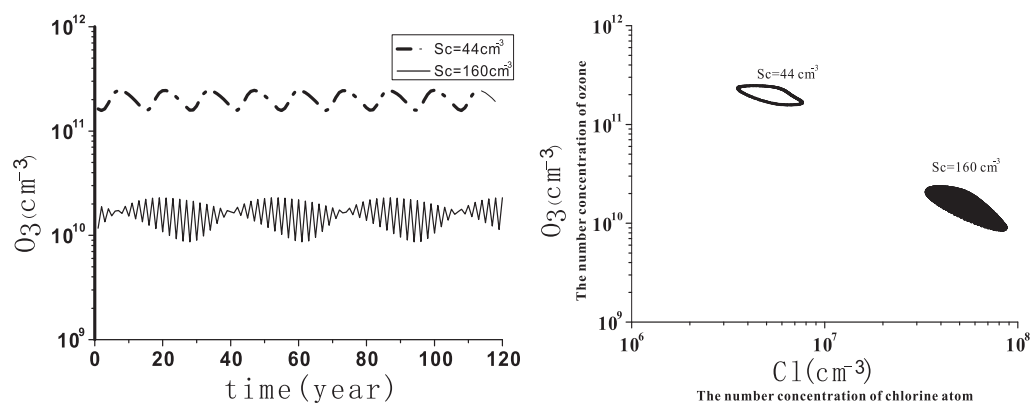


**Fig. 7.** Periodic solutions of ozone density dependence on the time obtained for  $S_{Cl} = 44 \text{ cm}^{-3} \text{ s}^{-1}$  and  $S_{Cl} = 160 \text{ cm}^{-3} \text{ s}^{-1}$ .

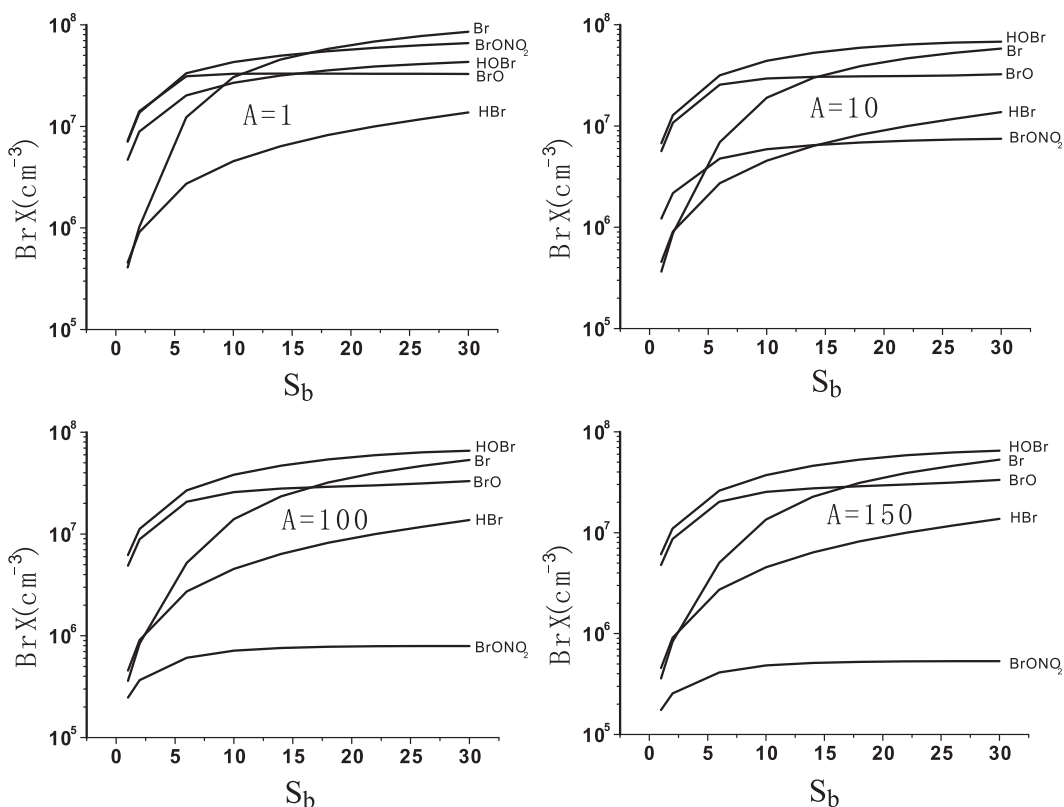


**Fig. 8.** Dependence of the states of the  $\text{Br}_x$  system on the aerosol surface area density  $A$  and the reactive bromide resource  $S_b$ .

A periodic solution of ozone density dependence on time for  $S_{Cl} = 44 \text{ cm}^{-3} \text{ s}^{-1}$  and  $S_{Cl} = 160 \text{ cm}^{-3} \text{ s}^{-1}$  when  $A = 100 \times 10^{-8} \text{ cm}^{-1}$  is provided in Fig. 7.

### 3.3 Response to the situation that both $S_b$ and $A$ change

Figure 8 shows the dependence of the states of the  $\text{Br}_x$  system on the aerosol surface area density  $A$  and the reactive bromide resource  $S_b$ , which shows the so-

lutions of the bromine family of this system when  $S_b$  is changing from 1 to 28 times, with  $A$  fixed at 1, 10, 100 and 150. It displays densities of bromine dependence with  $S_b$  and  $A$ . It is noted that densities of the bromine family enhance fast increasing of  $S_b$  firstly, then levels gradually. In different aerosol situations, it can be obviously seen that the heterogeneous chemical reaction influences  $\text{BrONO}_2$ , which notes that enhancing aerosol abundance can lead to a reduction in  $\text{BrONO}_2$

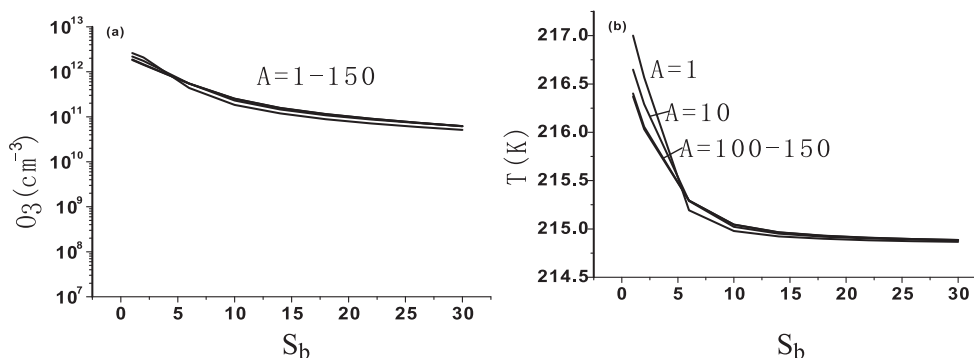


Fig. 9. Dependence of the states of the ozone system (a) and temperature (b) on  $A$  and the reactive bromide resource  $S_b$ .

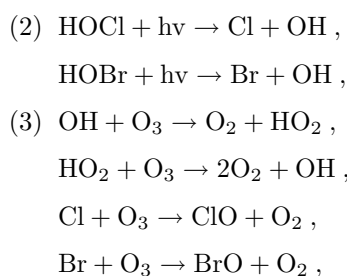
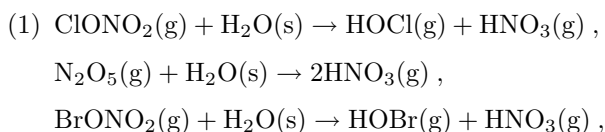
but an increase in HOBr.

For ozone in Fig. 9, the dependence of the states of the ozone system (a) and temperature (b) on  $A$  and the reactive bromide resource  $S_b$ , which shows the ozone concentration system when  $S_b$  is changing from 1 to 28 times, with  $A$  fixed at 1, 10, 100 and 150. One can see that the density of ozone depends with  $S_b$  and  $A$ , the density of ozone decreases monotonically, which indicates that bromide may play an important role in ozone destruction compared with nitrogen oxide and chloride oxide. Moreover, the adjustment through aerosol is not obvious in these cases. Also, temperature, shown in Fig. 9b, has a similar variability.

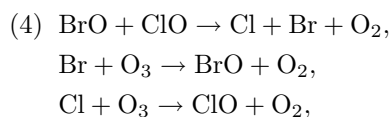
#### 4. Discussions

This paper improves the investigation (Wang and Yang, 2007) of nonlinear behavior of the lower stratospheric photochemical system in the context of natural and anthropogenic emissions of reactive nitrogen chlorine and bromine having increased rapidly in recent years (Fraser and Prather, 1999; WMO, 2007). In this paper, the bromine family is added and a radiation scheme is also considered in a simplified mechanism-based heterogeneous photochemical box model. The results of this study contribute to the theoretical analysis of the possible future behavior of atmospheric ozone in the lower mid-latitude stratosphere, under conditions of increasing external forcing strength by reactive nitrogen, chlorine and bromide under the framework of interaction between chemistry and radiation.

The net results caused by the heterogeneous chemistry are enhancing the reactive chlorine and the reactive bromide and reducing reactive nitrogen.



Due to the above reactions, for depleting ozone, the chlorine and bromine chemistry play more important roles than the nitrogen chemistry. In particular, it indicated that the above process should be strengthened with the increase in aerosol area density.



In addition, reactions between BrO and ClO may play an important role in ozone depletion, through Eq. (4) to convert  $2\text{O}_3 \rightarrow 3\text{O}_2$ ; therefore, much ozone is lost.

Moreover, introducing the temperature and ozone feedback effect in this box model did not change the topology of the ozone system; the stratospheric temperature change interplays with ozone number density. Actually, the existence of the nonlinear effects in the box model employed in these studies is conditioned by the presence of influxes and sinks of chemical constituents, which are due to transport processes. However, an analysis of the photochemistry within the framework of the box model suggests that the transport processes involved should be parameterized in the simplest manner.

**Acknowledgements.** This research was supported by the National Basic Research Program of China under Grant No. 2010CB428604 and the National Natural Science Foundation of China under Grant No. 41075061. We

are grateful to the two anonymous referees for their valuable suggestions.

## REFERENCES

- Bi, Y., Y. J. Chen, R. J. Zhou, M. J. Yi, and S. M. Deng, 2011: Simulation of the effect of watervapor increase on temperature in the stratosphere. *Adv. Atmos. Sci.*, **28**(4), 832–842, doi: 10.1007/s00376-010-0047-7.
- Bojkov, R. D. 1995: *The Changing Ozone Layer*. World Meteorological Organization and United Nations Environment Program, 24pp.
- Briegleb, B. P., 1992: Longwave band model for thermal radiation in climate studies. *J. Geophys. Res.*, **97**(D11), 11475–11485.
- Crutzen, P. J., 1996: My life with O<sub>3</sub>, NO<sub>x</sub>, and other YZO<sub>x</sub> compounds (Nobel lecture). *Angewandte Chemie International Edition*, **35**(16), 1758–1777.
- Fisher, D. A., and Coauthors, 1994: Production and emission of CFCs, Hallons, and related molecules. *Report on Concentrations, Lifetimes, and Trends of CFCs, Hallons, and Related Species*, National Aeronautics and Space Administration, Kaye et al., Eds., Washington D C, NASA Reference Publication, 248pp.
- Fraser, P. J., and M. J. Prather, 1999: Uncertain road to ozone recovery. *Nature*, **398**, 663–664.
- Gear, C. W., 1969: The automatic integration of stiff ordinary differential equations. *Information Processing 68*, A. J. H. Morrell, Ed., North Holland, Amsterdam, 187–193.
- Granier, C., and G. Brasseur, 1992: Impact of heterogeneous chemistry on model predictions of ozone changes. *J. Geophys. Res.*, **97**(D16), 18015–18033.
- Hanson, D. R., and K. Mauersberger, 1988: Laboratory studies of the nitric acid trihydrate: Implications for the south polar stratosphere. *Geophys. Res. Lett.*, **15**, 855–858.
- Hofmann, D. J., and S. Solomon, 1989: Ozone destruction through heterogeneous chemistry following the eruption of El Chichon. *J. Geophys. Res.*, **94**, 5029–5041.
- Hu, Y., F. Ding, and Y. Xia, 2009: Stratospheric climate trends under conditions of global climate changes. *Advance in Earth Sciences*, **24**(3), 242–251.
- Johnston, H. S., 1971: Reduction of stratospheric ozone by nitrogen oxide catalysts from supersonic transport exhaust. *Science*, **173**(3996), 517–522.
- Kononov, I. B., M. F. Alexander, and A.Y. Mukhina, 1999: Toward understanding of the nonlinear nature of atmospheric photochemistry: Multiple equilibrium states in the high-latitude lower stratospheric photochemical system. *J. Geophys. Res.*, **104**, 3669–3689.
- Li, G., R. Zhang, J. Fan, and X. Tie., 2005: Impacts of black carbon aerosol on photolysis and ozone. *J. Geophys. Res.*, **110**, D23206, doi: 10.1029/2005JD005898.
- McCormick, M. P., and R. E. Veiga, 1992: SAGE II measurement of early Pinatubo aerosols. *Geophys. Res. Lett.*, **19**, 155–158.
- Orlando, J. J., J. Burkholder, S. McKeen, and A. Ravishankara, 1991, Atmospheric fate of several hydrofluoroethanes and hydrochloroethanes. *J. Geophys. Res.*, **96**, 5013–5023.
- Potter, B., E. Holton, and R. James, 1995: The role of monsoon convection in the dehydration of the lower tropical stratosphere. *J. Atmos. Sci.*, **52**(8), 1034–1050.
- Prather, M. J., 1992: Catastrophic loss of stratospheric ozone in dense volcanic clouds. *J. Geophys. Res.*, **97**, 10187–10191.
- Rodriguez, J. M., K. W. Malcolm, and D. Nien, 1991: Role of heterogeneous conversion of N<sub>2</sub>O<sub>5</sub> on sulfuric aerosols in global ozone losses. *Nature*, **352**, 134–137.
- Theresa, H., and Coauthors, 1998: Description of SOCRATES-A chemical dynamical radiative two-Dimensional model. *NCAR Technical Note*, NCAR/TN-400+EDD.
- Tian, W. S., M. P. Chipperfield, and D. Lu, 2009: Impact of increasing stratospheric water vapor on ozone depletion and temperature change. *Adv. Atmos. Sci.*, **26**(3), 423–437, doi: 10.1007/s00376-009-0423-3.
- Tie, X. X., G. P. Brasseur, X. Lin, P. Friedlingstein, C. Granier, and P. J. Rasch, 1994: The impact of high altitude aircraft on the ozone layer in the stratosphere. *Journal of Atmospheric Chemistry*, **18**, 103–128.
- Tie, X., and G. P. Brasseur, 1996: The importance of heterogeneous bromine chemistry in the lower stratosphere. *Geophys. Res. Lett.*, **23**, 2505–2508.
- Tie, X., S. Chandra, J. R. Ziemke, C. Granier, and G. Brasseur, 2006: Satellite measurements of tropospheric column O<sub>3</sub> and NO<sub>2</sub> in eastern and southeastern Asia: Comparison with a Global Model (MOZART-2). *Journal of Atmospheric Chemistry*, **56**, doi: 10.1007/s10874-006-9045-7.
- Tolbert, M. A., M. J. Rossi, and D. M. Golden, 1988: Heterogeneous interactions of chlorine nitrate, hydrogen chloride, and nitric acid with sulfuric acid surfaces at stratospheric temperature. *Geophys. Res. Lett.*, **15**, 847–850.
- Wang, G., and P. Yang, 2006: On the nonlinear response of lower stratospheric ozone to NO<sub>x</sub> and ClO<sub>x</sub> perturbations for different CH<sub>4</sub> sources. *Adv. Atmos. Sci.*, **23**(5), 750–757.
- Wang, G., and P. Yang, 2007: On the nonlinear response of the lower stratospheric ozone to NO<sub>x</sub> and ClO<sub>x</sub> perturbations. *Chinese Journal of Geophysics*, **50**(1), 51–57.
- Weinberg, P. O., and Coauthors, 1994: Removal of stratospheric O<sub>3</sub> by radicals: in situ measurements of OH, HO<sub>2</sub>, NO, NO<sub>2</sub>, ClO, and BrO. *Science*, **266**(5184), 398–404.
- WMO, 2007: *Scientific Assessment of Ozone Depletion: 2006*. Global Ozone Research and Monitoring Project—Report. No. 50, Geneva, Switzerland.
- White, W. H., and D. Dietz, 1984: Does the photochem-

- istry of the troposphere admit more than one steady state. *Nature*, **309**(5965), 242–244.
- Yang, P. C., and G. Brasseur, 1994: Dynamics of the oxygen–hydrogen system in the mesosphere. Part 1. Photochemical equilibrium and catastrophe. *J. Geophys. Res.*, **99**(D10), 20955–20965.
- Yang, P. C., and G. Brasseur, 2001: The nonlinear response of stratospheric ozone to  $\text{NO}_x$  and  $\text{ClO}_x$  perturbations. *Geophys. Res. Lett.*, **28**(4), 717–720.
- Yang, P. C., and G. Brasseur, 2004: Mathematical analysis of the stratospheric photochemical system. *J. Geophys. Res.*, **109**, D15308.